Pergamon

Bioorganic & Medicinal Chemistry 9 (2001) 1721–1730

BIOORGANIC & MEDICINAL CHEMISTRY

Ligand Recognition by the Vitamin D Receptor

Mihwa Choi,[a] Keiko Yamamoto,[a,*] Hiroyuki Masuno,[a] Kinichi Nakashima,[b,†] Tetsuya Taga[b,†] and Sachiko Yamada[a,*]

[a]*Institute of Biomaterials and Bioengineering, Tokyo Medical and Dental University, 2-3-10, Surugadai Kanda, Chiyoda-ku, Tokyo 101-0062, Japan*

[b]*Medical Research Institute, Tokyo Medical and Dental University, 2-3-10, Surugadai Kanda, Chiyoda-ku, Tokyo 101-0062, Japan*

Received 23 January 2001; accepted 26 February 2001

Abstract—Three-dimensional structure of the ligand binding domain (LBD) of the vitamin D receptor (VDR) docked with the natural ligand 1α,25-dihydroxyvitamin D_3 [1,25-$(OH)_2D_3$] has been mostly solved by the X-ray crystallographic analysis of the deletion mutant (VDR-LBDΔ165-215). The important focus, from now on, is how the VDR recognizes and interacts with potent synthetic ligands. We now report the docking models of the VDR with three functionally and structurally interesting ligands, 22-oxa-1,25-$(OH)_2D_3$ (OCT), 20-epi-1,25-$(OH)_2D_3$ and 20-epi-22-oxa-24,26,27-trihomo-1,25-$(OH)_2D_3$. In parallel with the computational docking studies, we prepared twelve one-point mutants of amino acid residues lining the ligand binding pocket of the VDR and examined their transactivation potency induced by 1,25-$(OH)_2D_3$ and these synthetic ligands. The results indicate that L233, R274, W286, H397 and Y401 are essential for holding the all ligands tested, S278 and Q400 are not important at all, and the importance of S237, V234, S275, C288 and H305 is variable depending on the side-chain structure of the ligands. Based on these studies, we suggested key structural factors to bestow the selective action on OCT and the augmented activities on 20-epi-ligands. Furthermore, the docking models coincided well with our proposed active space-region theory of vitamin D based on the conformational analyses of ligands. © 2001 Elsevier Science Ltd. All rights reserved.

Introduction

The hormone, 1α,25-dihydroxyvitamin D_3 [1,25-$(OH)_2D_3$], plays a major role in calcium homeostasis, and it is also involved in cell differentiation, cell proliferation and the immune system.[1] The actions of 1,25-$(OH)_2D_3$ are mediated by the nuclear vitamin D receptor (VDR).[2] The VDR is a member of the nuclear receptor superfamily that includes the receptors for steroid, thyroid and retinoid hormones as well as orphan receptors whose natural ligands are unknown.[3] All of these nuclear receptors (NRs) are assumed to express their function by a common mechanism with which NRs regulate the transcription of their target genes. The VDR belongs to the subfamily 1 in the NR superfamily along with RAR, TR and PPAR.[4] In the presence of the cognate ligand, these receptors in subfamily 1 heterodimerize with RXR forming an active NR-RXR complex, which binds to the direct repeat of the target gene promoter and then recruits coactivators.[5] With the development of molecular biology in this field, the coactivation mechanism in NR signaling became known to us as follows.[6,7] NRs bound with the ligand recruit p160 and CBP/p300 coactivators. The complex of these two coactivators possesses intrinsic histone acetyl transferase (HAT) activity and remodels chromatin. After the remodeling of chromatin, NRs dissociate the complex of p160 and CBP/p300 and then recruit the DRIP/TRAP coactivator which has no HAT activity allowing the recruitment of the basal transcription factors (RNA polymerase II holoenzyme). Although the mechanism of the transcription of target genes is complicated as described above, it is clear that

*Corresponding authors. Tel.: +81-3-5280-8038; fax: +81-3-5280-8005; e-mail: yamamoto@i-mde.tmd.ac.jp; yamada@i-mde.tmd.ac.jp

†Present address: Department of Cell Fate Modulation, Institute of Molecular Embryology and Genetics, Kumamoto University, 2-2-1, Honjo, Kumamoto, 860-0811 Japan.

0968-0896/01/$ - see front matter © 2001 Elsevier Science Ltd. All rights reserved.
PII: S0968-0896(01)00060-8

the binding of the ligand to NR initiates a sequence of events resulting in the activation of gene transcription. Thus, for the rational design of the vitamin D analogues that are potent therapeutic agents, it is of great importance to understand the direct interaction between VDR and its various ligands and then the relationship between the interaction and vitamin D functions.

We have been continuing the study on the structure–function relationship of vitamin D.[8–12] First, our attention was directed to the side chain of vitamin D[13] because most of potent vitamin D analogues were modified at the side chain. Using the computer-aided conformational analysis and conformationally restricted synthetic vitamin D analogues, we found that the spatial region occupied by the vitamin D side chain is grouped into five areas, termed them A, G, EA, EG, and F, and proposed the active space group concept which explains the relationships between the spatial region of vitamin D side-chains and the biological activities.[8,10–12] This theory has been generally accepted as explaining the three-dimensional structure – activity relationships of almost all known vitamin D analogues.[12,14–16] As a next step, to discuss the structure–activity relationships of vitamin D based on the VDR-structure, we constructed and reported the three-dimensional (3D) structure of the ligand binding domain (LBD) of VDR by the homology modeling technique.[17] At nearly the same time, the crystal structure of a deletion mutant VDR-LBD engineered for crystallization was reported by Moras' group.[18] Our model was essentially the same as the crystal structure except for some detailed parts. Because the crystal structure was solved using the VDR-LBD lacking 51 amino acid residues (S165–P215) in the long loop 1–3, ambiguity still remains in the structure of the VDR-LBD.

To clarify the direct interaction between the VDR and its natural, as well as synthetic ligands, we made 12 one-point mutants of amino acid residues lining the ligand binding pocket (LBP), evaluated their transcriptional activity, and assigned the role of each amino acid residue in the hormone harboring. On the basis of this mutational analysis, the docking of functionally and structurally interesting vitamin D side-chain analogues into VDR-LBD was carried out. We also suggested, based on these models, the structural factors that potentiate these analogues and that discriminate among coactivators.

Results

Three-dimensional structure of VDR-LBD

All NRs display a common modular structure comprising six distinct domains with an evolutionary highly conserved DNA binding domain (DBD) and a moderately conserved LBD.[19] The LBD functions as a multifunctional domain. Besides the ligand holding, it is involved in dimerization and in the ligand-dependent transactivation. Since 1995, the crystallographic structures of NR-LBDs have been successively reported.[20–30] All of those crystal NR-LBDs were found to have a quite similar three-layered architecture consisting of 11 to 12 helices and one or two sets of β-sheets, in spite of about 20% or less identity in their amino acid sequences. A marked 3-D structural difference is located at loop 1–3 whose conservation is poor in various NRs in terms of the amino acid sequence, its length and consequently the 3-D structure. Furthermore, this loop of each NR is also poorly conserved among species. The biological significance and the role of this loop are interesting but not yet clear.

In the previous paper, we reported the model of VDR-LBD bound with 1,25-$(OH)_2D_3$ that has 11 helices and exhibits the same three-layered structure as other NR-LBDs (Fig. 1a).[17] The crystal structure reported by Moras et al. is quite similar to our model (Fig. 1b).[18] In fact, the (root mean square distance) RMSD of Cαs between the protein parts of our model and the crystal structure is 1.206 Å in 177 residues without loop 1–3, the β-strands, helix 6 (H6) and connecting loops in which the distance between Cαs is over 2.5 Å, indicating high similarity in both structures. The most striking difference arose from the different treatment of the poorly conserved long loop 1–3. In our model, Y143–Q223 in the loop 1–3 was eliminated because this part was impracticable to construct by homology. This elimination is not assumed to significantly affect the 3-D structure of the LBP. In the deletion mutant for the crystallization, S165–P215 in the same loop was deleted so that the loop 1–3 runs straight down between H3 and the β-strands like ER and PR in subfamily 3. In the crystal structures of RAR, TR and PPAR classified in the same subfamily 1, this loop goes around the β-strands. Therefore, this part of the crystal VDR remains ambiguous. Residues constituting the LBP are almost the same between the model and the crystal structure. In both structures, the central part of LBP is surrounded by hydrophobic residues, whereas two extremities, site 1 and site 2, are surrounded by hydrophilic residues.

The docking mode of 1,25-$(OH)_2D_3$ to VDR-LBD in our model is quite similar to that of the crystal structure. In both structures, the A-ring part of the ligand is anchored to site 1 and the side-chain part to site 2. We emphasize that three hydrophilic residues (S237, R274 and H397) forming hydrogen bonds with the biologically important 1α- and 25-hydroxyl groups of 1,25-$(OH)_2D_3$ were identical in both the model and the crystal structure. The difference is the A-ring and the side-chain conformations of 1,25-$(OH)_2D_3$ in LBP and the hydrogen bond partner of the 3β-hydroxyl group. The A-ring of 1,25-$(OH)_2D_3$ adopts an α-form in our model whereas it has a β-form in the crystals. Also the amino acid residue forming a hydrogen bond with the 3β-hydroxyl group of 1,25-$(OH)_2D_3$ was not specified in our model whereas S278 and Y143 form hydrogen bonds with the 3β-hydroxyl group in the crystals. Y143 is conserved only in mammals so that the hydrogen bond between this residue and the ligand is not assumed to be essential. Concerning the side chain conformation, we docked 1,25-$(OH)_2D_3$ with the most stable gauche(+) conformation at the dihedral angle of

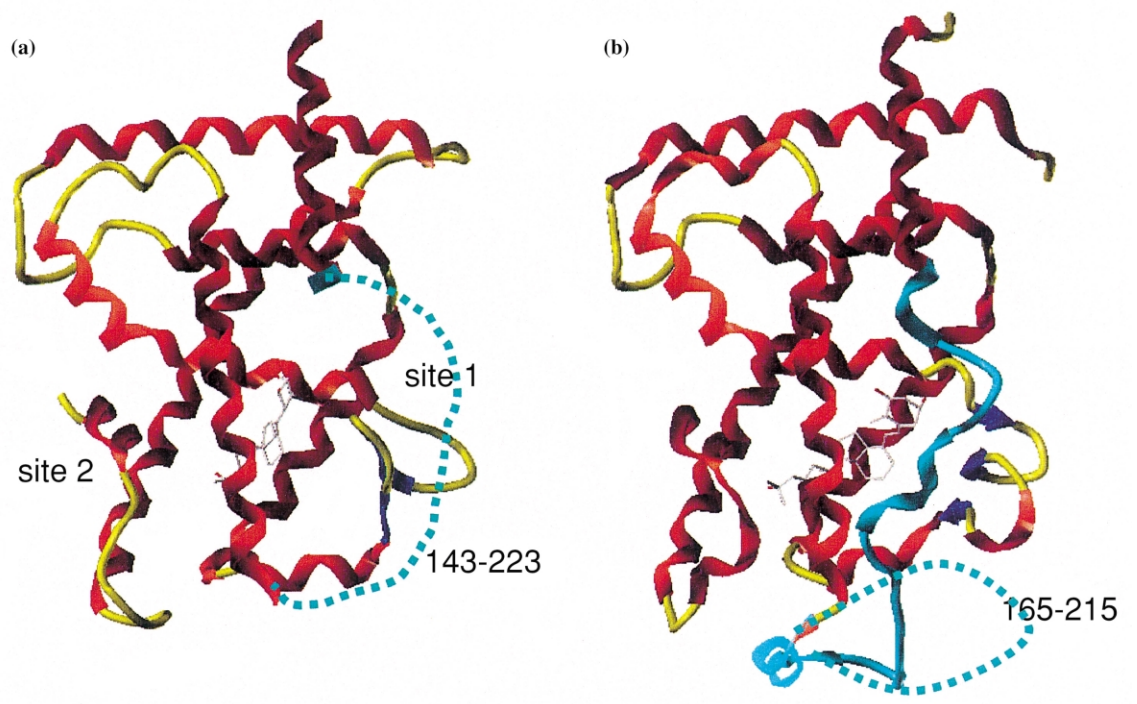

Figure 1. Three-dimensional structure of vitamin D receptor ligand binding domain (VDR-LBD). Ribbon presents α-helix and β-sheet and tube presents loop. Stick structure represents 1,25-$(OH)_2D_3$. (a) Constructed VDR-LBD. Amino acid residues between Y143 and Q223 were eliminated and depicted as a cyan dotted line. (b) Crystal structure of a deletion mutant VDR-LBD lacking residues between S165 and P215. Deleted region is depicted as a cyan dotted line.

C(16-17-20-22). Unexpectedly, in the crystals, the hormone adopts an unstable gauche(−) conformation at the same dihedral angle. We did not expect that the natural hormone would adopt an unstable conformation in its specific receptor, because the hormone and its specific receptor were assumed to cooperatively evolve to form the complex with a conformation favorable to each other.

Selection of amino acid residues for site-directed mutagenesis

There is no subtype of VDR different from other NRs such as RAR, TR, PPAR, ER and so on. In individual species, a unique VDR responds to the natural hormone, 1,25-$(OH)_2D_3$. Thus, we assumed that important amino acid residues for ligand harboring are conserved in all species. In addition, our 3-D model of VDR-LBD implied which residues interact with the ligand. Inspecting our model together with the conservation of the residues, we selected 12 residues of VDR for site-directed mutagenesis: L233, V234, and S237 at H3; R274, S275, and S278 at H5; W286 and C288 at the β-sheet; H305 at loop 6–7; and H397, Q400, and Y401 at H11 (Fig. 2). All of these residues are conserved in all species so far known and face LBP in VDR. We planned the replacement of each residue by alanine which is an amino acid with the smallest side chain. This substitution was expected to have little effect on the backbone structure of the parent protein, because the allowed dihedral angle (ϕ and ψ) at the main chain of alanine is generally the same in all other residues except for glycine and proline.

In the crystal structure, residues whose side-chains interact with other residues by intramolecular hydrogen bonds are R274, S275, W286, H305 and Q400. Guanidine of R274 interacts with T142 at the tail of H1 by a hydrogen bond which is conserved in NR subfamily 1 except for PPAR. We assumed that this bond is not necessarily essential because similar interaction was not observed in PPAR in subfamily 1[29,30] and NRs in other subfamilies.[20,25–28] The hydroxyl group of S275 forms hydrogen bonds with indole of W286, imidazole of H305 and the side chain carbonyl group of Q400. The Q400 side chain also forms a hydrogen bond with the hydroxyl group of S306. We assumed that these hydrogen bonds are not crucial for holding the 3-D structure of VDR because the mutants of S275 and Q400, that is, S275A and Q400A, had little effect on transactivation potency as described below. Thus, nine mutants, S237A, R274A, S275A, S278A, C288A, H305A, H397A, Q400A and Y401A, are assumed to have little effect on the folding of the 3-D structure of VDR. Mutants of nonpolar residues, L233A, V234A and W286A, decrease hydrophobic interaction with the ligand and/or intramolecular interaction with other residues and increase the volume of LBP.

Transactivation property of one-point mutant VDRs

We prepared 12 cDNA clones of one-point mutated full-length VDRs as described in Materials and Methods. To assess the levels and stability of these mutant VDRs, Western immunoblot analysis of these proteins was performed using the 9A7γ monoclonal anti-VDR antibody.[31] As shown in Figure 4A, the analysis

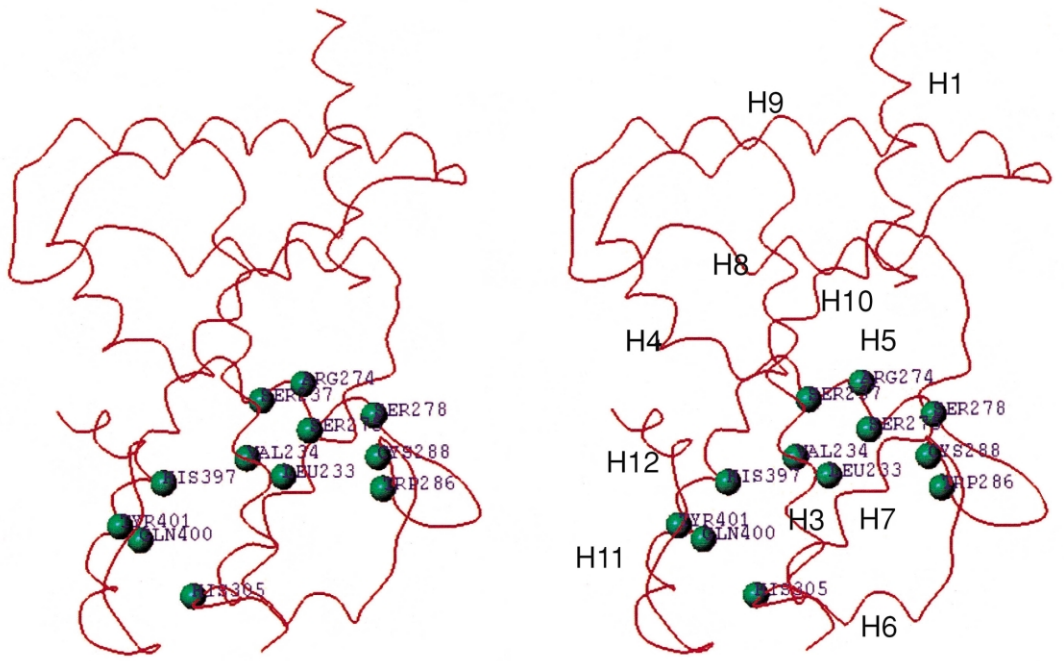

Figure 2. Amino acid residues lining the ligand binding pocket of VDR which were mutated to alanine (stereoview). Green balls represent Cαs of mutated residues.

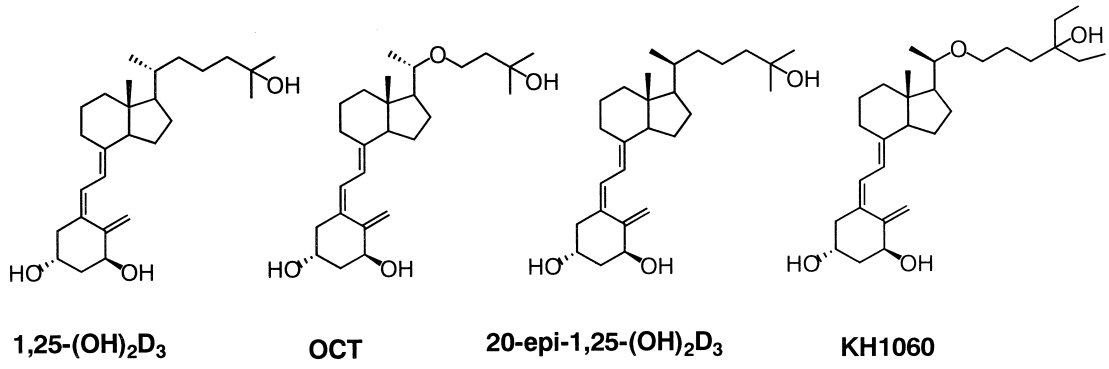

Figure 3. Structures of 1,25-$(OH)_2D_3$ and its analogues.

revealed a nearly equivalent expression of wild type and all one-point mutant VDRs indicating that these mutations have little effect on the expression and stability of the hVDR protein in COS-7 cells.

The transactivation potency of the wild type and the 12 one-point mutant VDRs was evaluated in COS-7 cells using a dual luciferase assay system. COS-7 cells were cotransfected with wild type or mutant hVDR expression plasmid, a reporter plasmid containing mouse osteopontin VDRE[32] and the internal control plasmid, and then stimulated with a natural hormone or the three representative side-chain analogues, 22-oxa-1,25-$(OH)_2D_3$ (OCT),[33] 20-epi-1,25-$(OH)_2D_3$[34] and 20-epi-22-oxa-24,26,27-trihomo-1,25-$(OH)_2D_3$ (KH1060).[34] The results are shown in Figure 4B–E.

Activity induced by 1,25-$(OH)_2D_3$ was completely abolished by the five mutants L233A, R274A, W286A, H397A, and Y401A, moderately reduced by the mutants V234A, S237A, S275A, C288A, and H305A, and little affected by S278A and Q400A. Thus, five residues, L233, R274, W286, H397, and Y401, are found to be essential for hormone harboring.

As shown in Figure 4C, the transactivation spectrum of OCT was quite similar to that of the natural hormone except for the mutant V234A. V234A stimulated by OCT showed the same activity as the wild type, although that by 1,25-$(OH)_2D_3$ showed reduced activity (Fig. 4B, C). 20-Epi-1,25-$(OH)_2D_3$ and KH1060 showed stronger transcriptional activity than the 20-normal compounds, 1,25-$(OH)_2D_3$ and OCT. The activity of 20-epi-ligands already reached a maximum at 10^{-8} M concentration. Thus, we evaluated the activity at 10^{-10} M concentration of these two ligands (Fig. 4D, E). Two 20-epi ligands showed a different transactivation pattern from the 20-normal vitamins. S275A mutant induced by 20-epi-1,25-$(OH)_2D_3$ increased its activation potency compared to the wild type, and H305A mutant was little affected. In the stimulation with KH1060, two more mutants of S237A and C288A,

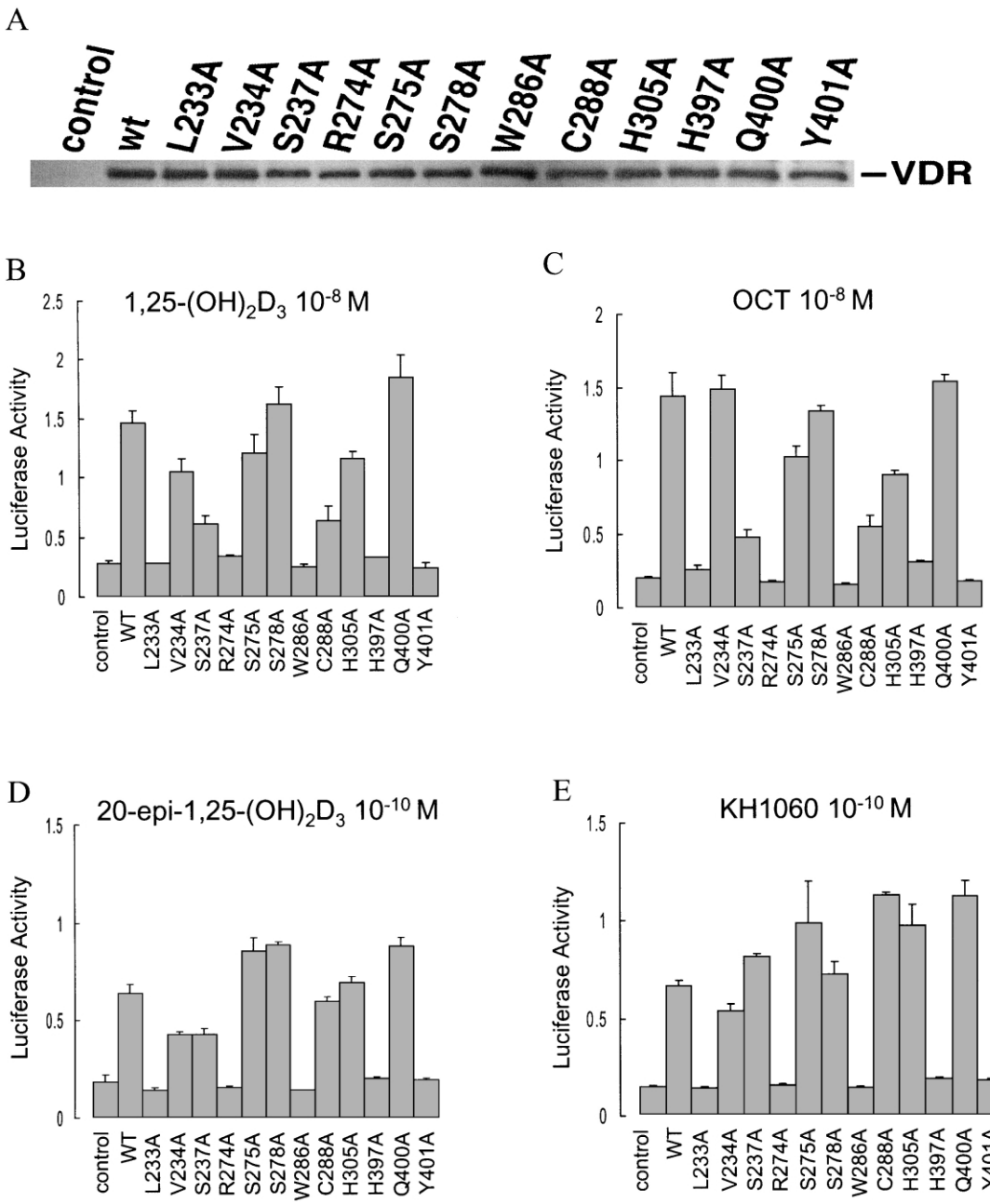

Figure 4. Immunoblot analysis and transactivation of 12 one-point mutant VDRs. (A) Expression of wild type and mutant VDRs determined by immunoblot analysis. (B-E) Transactivation potency induced by 10^{-8} M of 1,25-$(OH)_2D_3$ (B), 10^{-8} M of OCT (C), 10^{-10} M of 20-epi-1,25-$(OH)_2D_3$ (D), and 10^{-10} M of KH1060 (E).

in addition to S275A and H305A, increased their potency. It should be emphasized that the five mutants, L233A, R274A, W286A, H397A, and Y401A, that abolished 1,25-$(OH)_2D_3$ dependent transcriptional activity, also significantly reduced the induction by all these analogues.

Role of amino acid residues and docking of 1,25-$(OH)_2D_3$

We assumed the role of the important amino acids as follows (Table 1) Around the A-ring of the natural hormone, R274 and S237 together form a pincer-type hydrogen bond with the 1α-hydroxyl group (Fig. 5A). R274 plays a crucial role and S237 plays an assistant role. It is known that a natural mutant R274L causes hereditary vitamin D-resistant rickets (HVDRR).[35] In our experiment using the full-length VDR, the mutant of S278A did not affect 1,25-$(OH)_2D_3$ binding and the transactivation, whereas the mutant of C288A significantly decreased 1,25-$(OH)_2D_3$ binding and the transactivation.[17] From this fact together with the result of affinity labeling experiment by Ray et al.,[36] we assigned that wild type VDR interacts with 3β-hydroxyl group of 1,25-$(OH)_2D_3$ through C288 but not S278, although in the crystal structure, S278 forms a hydrogen bond with the 3β-hydroxyl group. If the A-ring of 1,25-$(OH)_2D_3$ adopts an α-form in contrast with the β-form

Table 1. Functions of amino acid residues lining the LBP of VDR

1,25-$(OH)_2D_3$	Amino acid residue	Natural mutant	Location	Assumed function
A-ring	S237		H3	Assistant hydrogen bond with 1α-OH
	R274	R274L	H5	Hydrogen bond with 1α-OH
	S278		H5	Hydrogen bond with 3β-OH (crystal of mutant VDR)
	C288		β-sheet	Hydrogen bond with 3β-OH (our model)
B- and C-ring	L233	L233fs	H3	Hydrophobic interaction with ligand
	W286		β-sheet	Hydrophobic interaction with ligand
D-ring and side chain	V234		H3	Hydrophobic interaction with ligand
	H305	H305Q	loop 6-7	Assistant hydrogen bond with 25-OH (crystal of mutant VDR)
	H397		H11	Hydrogen bond with 25-OH
	Y401		H11	Hydrophobic interaction with H12

in the crystal structure, the 3β-hydroxyl group is able to interact directly with C288. Thus, we assume that the A-ring of 1,25-$(OH)_2D_3$ adopts an α-form in the wild type VDR to contact C288 through the 3β-hydroxyl group as previously reported.[17]

At the seco-B- to C-ring part, W286 and L233 together hold the hydrophobic core part of the hormone from both bottom and top sides by hydrophobic interaction. At the terminal 25-hydroxyl group of the side chain, H397 strongly anchors the 25-hydroxyl group together with H305 which is assumed to play an assistant role. Y401 at the tail of H11 is important, probably in folding H12 in the active form by hydrophobic interaction with a lipophilic residue at H12. A natural frameshift mutant, L233fs, which causes the truncation of the VDR, and a one-point mutant H305Q are also known in HVDRR.[37,38] The hydrophobic D-ring to the side-chain part was found to be surrounded by hydrophobic residues: L230 and V234 at H3; I268, I271 and M272 at H5; V300 and A303 at H6; and L309 and L313 at H7. V300, L309 and L313 which are conserved in all species surround the C(21)H_3 of 1,25-$(OH)_2D_3$. It is likely that the hydrophobic interaction between these three residues and C(21)H_3 is important in ligand harboring and that this interaction overcomes the unfavorable conformation at C(16-17-20-22) of 1,25-$(OH)_2D_3$.

Docking manner of vitamin D side-chain analogues

As described above, the crystal structure of VDR-LBD was assumed to be unimpaired except for the surroundings of the A-ring of 1,25-$(OH)_2D_3$. Therefore, we used the coordinates of the crystal structure of the VDR-LBD for the following docking study.

22-Oxa-1,25-$(OH)_2D_3$ (OCT). The transactivation spectrum of OCT indicates that this ligand binds to VDR in the same manner as the natural hormone. We docked OCT to VDR-LBD by superimposing the A- to D-ring of OCT on that of 1,25-$(OH)_2D_3$ in the LBD (Fig. 5B). The structural difference between OCT and 1,25-$(OH)_2D_3$ is only at the 22-position: sp^3-oxygen occupies the 22-position of OCT instead of C(22)H_2 of 1,25-$(OH)_2D_3$. In the crystal structure, the C(22)H_2 of 1,25-$(OH)_2D_3$ has a hydrophobic interaction with V234 (4.3 Å) and I268 (4.3 Å). Replacement of this CH_2 with oxygen would significantly reduce this interaction. The transactivation potency of V234A mutant stimulated by 1,25-$(OH)_2D_3$ was reduced compared with wild type VDR, whereas that by OCT was little affected. These results show that the C(22)H_2 of 1,25-$(OH)_2D_3$ favorably interact with V234, whereas OCT can not have this favorable interaction. The fact that the VDR affinity of OCT is eight times less potent than 1,25-$(OH)_2D_3$[39] can be explained by the lack of this favorable hydrophobic interaction.

It should be noted that OCT can be harbored in VDR with the stable gauche(−) conformation at C (16-17-20-22). The dihedral angle at C(16-17-20-22) determines the direction of the vitamin D side chain to the A, G, EA, EG or F regions. All of the vitamin D analogues categorized in the F region such as OCT, 16-ene-1,25-$(OH)_2D_3$ derivatives and 18-nor-1,25-$(OH)_2D_3$, can bind to VDR with their stable gauche(−) conformation. This fact may explain why they have high potency.

20-Epi-1,25-$(OH)_2D_3$. Though 20-epi-1,25-$(OH)_2D_3$ showed higher activity than 1,25-$(OH)_2D_3$, the transactivation spectrum is similar to 1,25-$(OH)_2D_3$ except for the mutants of S275A and H305A, which are not crucial residues for the ligand holding as described above. Thus, we docked 20-epi-1,25-$(OH)_2D_3$ into VDR-LBD in a manner similar to that of 1,25-$(OH)_2D_3$. It should be noted that 20-epi-1,25$(OH)_2D_3$ can bind to the VDR with its stable conformation at C(16-17-20-22) (Fig. 5C). We can speculate an answer to the question of why the affinity for VDR of 20-epi-1,25-$(OH)_2D_3$ is higher than that of the natural hormone. The answer is (i) 20-epi-1,25-$(OH)_2D_3$ can be harbored in the LBP with its stable side-chain conformation, (ii) C(22)H_2 of 20-epi-1,25-$(OH)_2D_3$ can adopt a quite favorable position for van der Waals contact with V300 at H6. In fact, the distance between the C(22) and C(γ) of V300 is 3.3 Å in the docking model.

20-Epi-22-oxa-24,26,27-trihomo-1,25-$(OH)_2D_3$ (KH1060). In the case of KH1060, two additional mutants of S237A and C288A showed higher potency than the wild type. This suggests that S237 and C288 do not interact with the 1α-hydroxyl and 3β-hydroxyl groups of KH1060, respectively. Thus, the A-ring conformation of KH1060 in LBP may be different from that of the natural hormone. We speculate that the A-ring of KH1060 adopts a β-form in VDR-LBD, resulting in the disruption of the weak hydrogen bond between S237 and the 1α-hydroxyl group (Fig. 5D). The strong biological

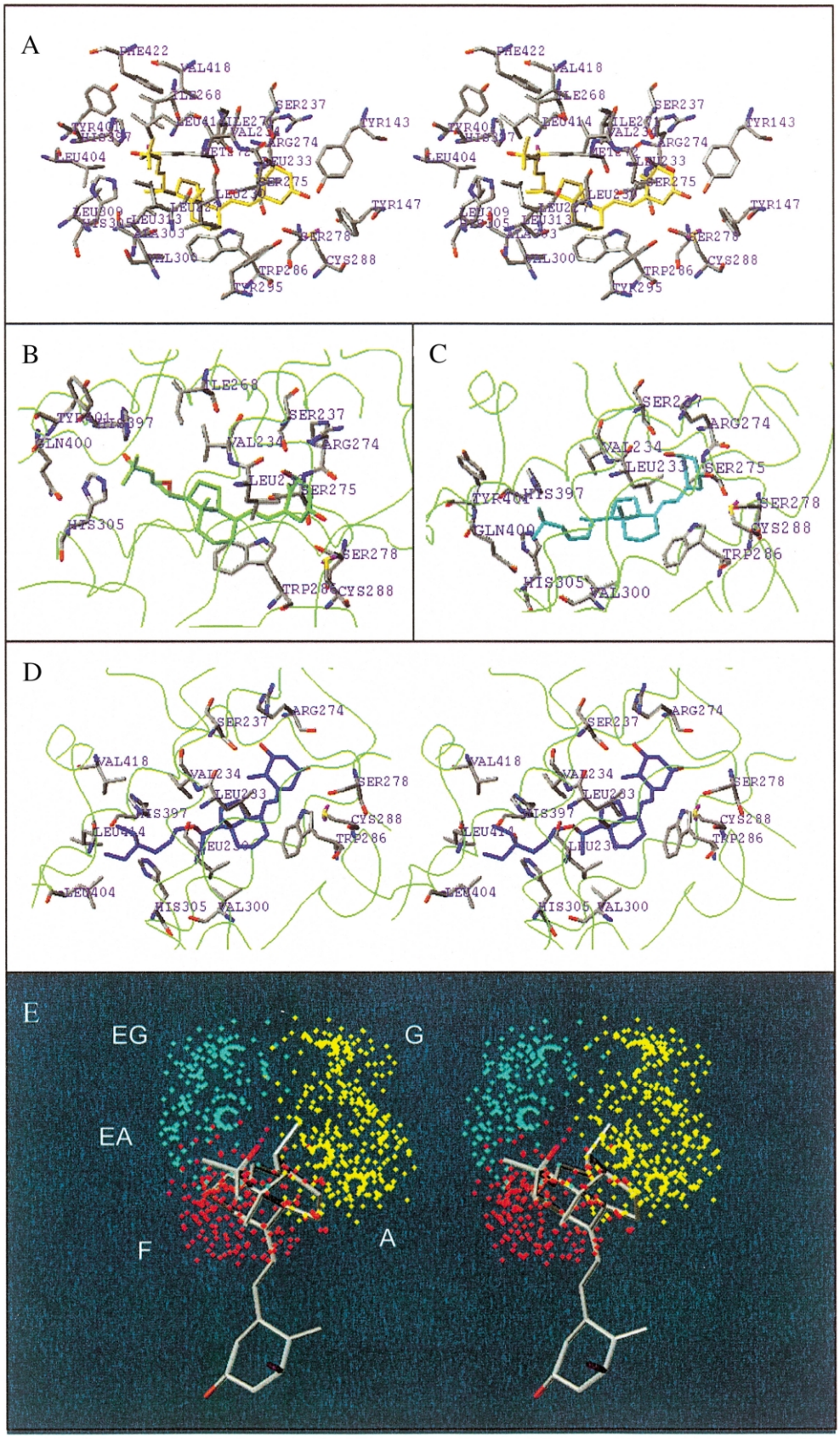

Figure 5. Docking model of the ligand with VDR-LBD (A-D) and superposition of 1,25-$(OH)_2D_3$ with the active conformation on the dot map (E). Docking model of (A) 1,25-$(OH)_2D_3$ (yellow), (B) OCT (green), (C) 20-epi-1,25-$(OH)_2D_3$ (cyan) and (D) KH1060 (blue). (E) 1,25-$(OH)_2D_3$ in the VDR-LBD was superimposed on the dot map of the vitamin D side chain. Dots show the regions which the 25-oxygen of the vitamin D side chain can occupy. Yellow dots show the A and G regions, and cyan dots show the EA and EG regions. Red dots represents the F region. (A), (D) and (E) are stereoviews.

activity of KH1060 is explained by the following structural features. (i) KH1060 adopts a stable gauche(−) conformation at C(16-17-20-22) because of oxygen instead of $C(22)H_2$. (ii) One CH_2 elongation between C(20) and C(25) increases the hydrophobic interaction with H3. (iii) Two methyl groups at C(26) and C(27) reinforce the interaction with L404 at H11 and with L414 and V418 at H12.

Ligand in VDR-LBP and dot map

We have reported that the spatial region occupied by the side chains of 1,25-$(OH)_2D_3$ and its analogues is categorized into five areas. These areas are visually distinguished by creating a dot map in which dots indicate the position of the 25-oxygen of the ligand. Furthermore, we suggested that the A, EA and F regions are important for vitamin D to have high potency. We superposed 1,25-$(OH)_2D_3$ in the VDR on the dot map of the vitamin D side-chain (Fig. 5E). This picture reveals that the 25-hydroxyl group of 1,25-$(OH)_2D_3$ in the VDR-LBD is located at the boundary region of the A, F and EA regions. Thus, our active space region theory derived based on the ligand conformations successfully predicted the correct position of the 25-hydroxyl group in the VDR in addition to assuming the side-chain structure of high potency.

Discussion

OCT was found to be the first compound having a potent differentiating activity with low calcemic activity.[40] Much attention has been focused on the molecular mechanism for the selective actions of OCT. It has been reported that OCT differs from the parent 1,25-$(OH)_2D_3$ in its pharmacokinetics,[41] intracellular metabolism,[42,43] and non-genomic actions.[44] It has also been reported that selective recruitment of cofactors by the VDR stimulated with OCT may be responsible for the selective actions.[45] Our mutational analysis and the docking study showed that OCT is different from 1,25-$(OH)_2D_3$ only with respect to the absence of the interaction between the 22-oxygen and the hydrophobic residues (V234 and I268). Probably, the absence of this interaction reduces the affinity for VDR. Recently, it has been reported that a van der Waals interaction between H5 and H3 of the mineralocorticoid receptor is induced by the ligand binding and that this interaction is highly conserved among diverse NRs.[46] This interaction is assumed to be important for NR-activation by the bending of H3 which forms a surface for cofactor binding together with H12. In the case of the VDR, I271 at H5 interacts with V234 at H3 by 1,25-$(OH)_2D_3$ binding. The lack of the interaction between the important residue of V234 at H3 and OCT may explain why the VDR activated by OCT causes a different recruitment of the cofactors.

The 20-epi analogues of 1,25-$(OH)_2D_3$ are interesting agents because they show strong biological activities in spite of the unnatural stereochemistry at C(20).[34] Differential interaction of 1,25-$(OH)_2D_3$ and the 20-epi analogues with VDR has been reported on the basis of the proteolytic digestion analysis by Peleg.[47] Vanleeuwen also reported that KH1060 increases VDR stability in Ros 17/2.8 cells and that this ligand showed a far more dramatic protection of the VDR against proteolytic degradation compared with 1,25-$(OH)_2D_3$.[48] These findings indicate that the 20-epi analogues keep VDR forming the active complex, which is energetically stable and resistant to proteolysis. The 3-D model of 20-epi-ligand/VDR complexes explains these results. The model structure of the 20-epi-1,25-$(OH)_2D_3$/VDR complex suggests the stable conformation of the ligand as well as the ideal hydrophobic interaction between $C(22)H_2$ of the ligand and V300. The KH1060/VDR model reveals a considerably increased van der Waals contact in comparison with the 1,25-$(OH)_2D_3$/VDR complex. Probably, VDR including KH1060 is fixed to the active form through this strong van der Waals contact.

These studies led us to know that vitamin D compounds having increased hydrophobic interaction with the residues lining VDR-LBP, especially H12, in addition to bearing the potential hydrogen bonding groups at C(1), C(3), and C(25), can be expected to have potent biological activities. In fact, we found that 22*R*-methylation of 20-epi-1,25-$(OH)_2D_3$ augments the affinity for VDR by four times compared to the parent 20-epi-1,25-$(OH)_2D_3$.[10] It has also been reported that 2α-methylation of 1,25-$(OH)_2D_3$ increases the VDR affinity.[49] These results are likely due to the augmentation of hydrophobic interaction with the VDR.

In conclusion, we analyzed the docking manner of 1,25-$(OH)_2D_3$ as well as some interesting side-chain analogues in VDR-LBP based on the mutational studies and discussed how each ligand exhibits characteristic actions. Now the stage is set for rational design of vitamin D compounds based on the 3-D structure of the VDR.

Experimental

Site-directed mutagenesis

The human VDR (hVDR) expression vector pCMX-hVDR[50] was used as a template for in vitro site-directed mutagenesis. Point mutants were created using a QuickChange Site-directed Mutagenesis Kit (Stratagene, CA, USA). Twelve clones of mutated hVDRs (L233A, V234A, S237A, R274A, S275A, S278A, W286A, C288A, H305A, H397A, Q400A and Y401A) were produced by replacing the corresponding amino acid residue with alanine as described by the manufacturer. *E. coli* DH5α competent cells were transformed with the vectors incorporating the desired mutations. The cDNAs of the clones were purified by Qiagen Plasmid Midi-Kit (Qiagen, Valencia, CA, USA) and sequenced completely to ensure that no other base changes were produced by cycle sequencing.

Transfection and transactivation assay

COS-7 cells were cultured in Dulbecco's modified Eagle's medium (DMEM) supplemented with 5% fetal

calf serum (FCS). Cells were seeded on 24-well plates at a density of 2×10^4 per well. After 24 h, the cells were transfected with a reporter plasmid containing three copies of the mouse osteopontin VDRE (SPPx3-TK-Luc), a wild-type or mutant hVDR expression plasmid (pCMX-hVDR), and the internal control plasmid containing sea pansy luciferase expression constructs (pRL-CMV) by the lipofection method as described previously.[17] After 4 h-incubation, the medium was replaced with fresh DMEM containing 1% FCS. The next day, the cells were treated with either 10^{-8} M 1,25-$(OH)_2D_3$, 10^{-8} M OCT, 10^{-10} M 20-epi-1,25-$(OH)_2D_3$, 10^{-10} M KH1060 or ethanol vehicle and cultured for 18 h. Cells in each well were harvested with a cell lysis buffer, and the luciferase activity was measured with a luciferase assay kit (Toyo Ink, Inc., Japan) according to the manufacturer's instructions. Transactivation measured by the luciferase activity was normalized with the internal control. All experiments were done in triplicate.

Western immunoblot analysis

COS-7 cells maintained in DMEM with 5% FCS were seeded in 60-mm dishes at a density of 8×10^5 per dish. After 24 h, the cells were transfected with a wild-type or mutant hVDR expression plasmid (pCMX-hVDR) by the lipofection method as described above. After 4h-incubation, the medium was replaced with fresh DMEM containing 1% FCS. On the following day, the transfected cells were solubilized with Nonidet P-40 (NP-40) lysis buffer (0.5% NP-40/10 mM Tris–HCl, pH 7.6/150 mM NaCl/5 mM EDTA/2 mM Na_3VO_4/1 mM phenylmethylsulfonyl fluoride/5 μg of aprotinin per mL). The lysate was diluted 1.3 times in a sample buffer (4% SDS/ 4% β-mercaptoethanol/125 mM Tris–HCl, pH 6.8/0.002% BPB/ 20% glycerol) and boiled for 2 min. Then 15–20 μg of cellular protein was loaded on 4–20% Multi SDS-polyacrylamide gels (Daiichi Pure Chemicals, Tokyo). After electrophoretic fractionation, the proteins were electrotransferred to PVDF transfer membranes (Amersham, Hybond-P) using a Transblot apparatus (Bio-Rad) in 25 mM Tris–HCl, pH 7.4/ 192 mM glycine/20% methanol. The membrane was blocked by treating with 5% skim milk (Difco) in TBST buffer (25 mM Tris, 136 mM NaCl, 2 mM KCl, 0.05% Tween 20) for 40 min and was washed three times. The membrane was treated with the primary antibody (9A7γ monoclonal anti-VDR antibody) in TBST buffer for 1 h and washed four times.[31] The membrane was then incubated for 30 min with goat anti-rat IgG HRP-conjugated secondary antibody (Santa Cruz) in TBST buffer and washed four times. hVDR proteins were visualized by chemiluminescence using the Chemiluminescence Reagent (NEN™ Life Science Products, Inc.) according to the manufacturer's instructions.

Ligand docking and graphical manipulations. Ligand docking to VDR-LBD and graphical manipulations were performed using SYBYL 6.5 (Tripos, St. Louis). The atomic coordinates of the crystal structures of deletion mutant VDR-LBD as well as other NR-LBDs were retrieved from the Protein Data Bank (Research Collaboratory for Structural Bioinformatics). Vitamin D analogues were manually docked into VDR-LBD.

Acknowledgements

The authors thank Dr. L. Binderup of Leo Company for the generous gift of 20-epi-1,25-$(OH)_2D_3$ and KH1060. We thank also Dr. N. Kubodera of Chugai Pharmaceutical Co., Ltd., for the generous gift of OCT. We are grateful to Dr. J. Akai for help in the measurement of luciferase activity. This work was supported in part by research grants from the Atsuko Ouchi Memorial Fund, Tokyo Medical and Dental University.

References

1. Feldman, D., Glorieux, F. H., Pike, J. W. Eds. *Vitamin D;* Academic Press, 1997.
2. DeLuca, H. F. *J. Bone Miner. Metab.* **1990**, *8*, 1.
3. Evans, R. M. *Science* **1988**, *240*, 889.
4. Laudet, V.; Hanni, C.; Coll, J.; Catzeflis, F.; Stehelin, D. *EMBO J.* **1992**, *11*, 1003.
5. Forman, B. M.; Umesono, K.; Chen, J.; Evans, R. M. *Cell* **1995**, *81*, 541.
6. Freedman, L. P. *Cell* **1999**, *97*, 5.
7. Rachez, C.; Freedman, L. P. *Gene* **2000**, *246*, 9.
8. Yamamoto, K.; Ohta, M.; DeLuca, H. F.; Yamada, S. *Bioorg. Med. Chem. Lett.* **1995**, *5*, 979.
9. Ishida, H.; Shimizu, M.; Yamamoto, K.; Iwasaki, Y.; Yamada, S.; Yamaguchi, K. *J. Org. Chem.* **1995**, *60*, 1828.
10. Yamamoto, K.; Sun, W-Y.; Ohta, M.; Hamada, K.; DeLuca, H. F.; Yamada, S. *J. Med. Chem.* **1996**, *39*, 2727.
11. Yamada, S.; Yamamoto, K.; Masuno, H.; Ohta, M. *J. Med. Chem.* **1998**, *41*, 1467.
12. Yamamoto, K.; Ooizumi, H.; Umesono, K.; Verstuyf, A.; Bouillon, R.; DeLuca, H. F.; Shinki, T.; Suda, T.; Yamada, S. *Bioorg. Med. Chem. Lett.* **1999**, *9*, 1041.
13. Yamamoto, K.; Takahashi, J.; Hamano, K.; Yamada, S.; Yamaguchi, K.; DeLuca, H. F. *J. Org. Chem.* **1993**, *58*, 2530.
14. Van Haver, D.; De Clercq, P. J. *Bioorg. Med. Chem. Lett.* **1998**, *8*, 1029.
15. Zhou, X.; Zhu, G. D.; Van Haver, D.; Vandewalle, M.; De Clercq, P. J.; Verstuyf, A.; Bouillon, R. *J. Med. Chem.* **1999**, *42*, 3539.
16. Yamada, S.; Yamamoto, K.; Masuno, H. *Curr. Pharm. Des.* **2000**, *6*, 733.
17. Yamamoto, K.; Masuno, H.; Choi, M.; Nakashima, K.; Taga, T.; Ooizumi, H.; Umesono, K.; Sicinska, W.; Van-Hooke, J.; DeLuca, H. F.; Yamada, S. *Proc. Natl. Acad. Sci. U.S.A.* **2000**, *97*, 1467.
18. Rochel, N.; Wurtz, J. M.; Mitschler, A.; Klaholz, B.; Moras, D. *Molecular Cell* **2000**, *5*, 173.
19. Mangelsdorf, D. J.; Thummel, C.; Beato, M.; Herrlich, P.; Schutz, G.; Umesono, K.; Blumberg, B.; Kastner, P.; Mark, M.; Chambon, P.; Evans, R. M. *Cell* **1995**, *83*, 835.
20. Bourguet, W.; Ruff, M.; Chambon, P.; Gronemeyer, H.; Moras, D. *Nature* **1995**, *375*, 377.
21. Renaud, J. P.; Rochel, N.; Ruff, M.; Vivat, V.; Chambon, P.; Gronemeyer, H.; Moras, D. *Nature* **1995**, *378*, 681.
22. Klaholz, B. P.; Renaud, J. P.; Mitschler, A.; Zusi, C.; Chambon, P.; Gronemeyer, H.; Moras, D. *Nat. Struct. Biol.* **1998**, *5*, 199.
23. Wagner, R. L.; Apriletti, J. W.; McGrath, M. E.; West, B. L.; Baxter, J. D.; Fletterick, R. *Nature* **1995**, *378*, 690.

24. Darimont, B. D.; Wagner, R. L.; Apriletti, J. W.; Stallcup, M. R.; Kushner, P. J.; Baxter, J. D.; Fletterick, R. J.; Yamamoto, K. R. *Genes Dev*. **1998**, *12*, 3343.
25. Brzozowski, A. M.; Pike, A. C.; Dauter, Z.; Hubbard, R. E.; Bonn, T.; Engstrom, O.; Ohman, L.; Greene, G. L.; Gustafsson, J. A.; Carlquist, M. *Nature* **1997**, *389*, 753.
26. Tanenbaum, D. M.; Wang, Y.; Williams, S. P.; Sigler, P. B. *Proc. Natl. Acad. Sci. U.S.A*. **1998**, *95*, 5998.
27. Shiau, A. K.; Barstad, D.; Loria, P. M.; Cheng, L.; Kushner, P. J.; Agard, D. A.; Greene, G. L. *Cell* **1998**, *95*, 927.
28. Williams, S. P.; Sigler, P. B. *Nature* **1998**, *393*, 392.
29. Nolte, R. T.; Wisely, G. B.; Westin, S.; Cobb, J. E.; Lambert, M. H.; Kurokawa, R.; Rosenfeld, M. G.; Willson, T. M.; Glass, C. K.; Milburn, M. V. *Nature* **1998**, *395*, 137.
30. Uppenberg, J.; Svensson, C.; Jaki, M.; Bertilsson, G.; Jendeberg, L.; Berkenstam, A. *J. Biol. Chem*. **1998**, *273*, 31108.
31. Pike, J. W.; Marion, S. L.; Donaldson, C. A.; Haussler, M. R. *J. Biol. Chem*. **1983**, *258*, 1289.
32. Noda, M.; Vogel, R. L.; Craig, A. M.; Prahl, J.; DeLuca, H. F.; Denhardt, D. T. *Proc. Natl. Acad. Sci. U.S.A*. **1990**, *87*, 9995.
33. Murayama, E.; Miyamoto, K.; Kubodera, N.; Mori, T.; Matsunaga, I. *Chem. Pharm. Bull*. **1986**, *34*, 4410.
34. Binderup, L.; Latini, S.; Binderup, E.; Bretting, C.; Calverley, M.; Hansen, K. *Biochem. Pharmacol*. **1991**, *42*, 1569.
35. Kristjansson, K.; Rut, A. R.; Hewison, M.; O'Riordan, J. L. H.; Hughes, M. R. *J. Clin. Invest*. **1993**, *92*, 12.
36. Swamy, N.; Ray, R. First International Conference on Chemistry and Biology of Vitamin D Analogues, September 26–28, 1999, Providence, RI.
37. Cockerill, F. J.; Hawa, N. S.; Yousaf, N.; Hewison, M.; O'Riordan, J. L.; Farrow, S. M. *J. Clin. Endocrinol. Metab*. **1997**, *82*, 3156.
38. Malloy, P. J.; Eccleshall, T. R.; Gross, C.; Van Maldergem, L.; Bouillon, R.; Feldman, D. *J. Clin. Invest*. **1997**, *99*, 297.
39. Okano, T.; Tsugawa, N.; Masuda, S.; Takeuchi, A.; Kobayashi, T.; Nishii, Y. *J. Nutr. Sci. Vitaminol*. **1989**, *35*, 529.
40. Abe, J.; Morikawa, M.; Miyamoto, K.; Kaiho, S.; Fukushima, M.; Miyaura, C.; Abe, E.; Suda, T.; Nishii, Y. *FEBS. Lett*. **1987**, *226*, 58.
41. Brown, A. J.; Finch, J.; Grieff, M.; Ritter, C.; Kubodera, N.; Nishii, Y.; Slatopolski, E. *Endocrinology* **1993**, *133*, 1158.
42. Kamimura, S.; Gallieni, M.; Kubodera, N.; Nishii, Y.; Brown, A. J.; Slatopolski, E.; Dusso, A. *Endocrinology* **1993**, *133*, 2719.
43. Bikle, D. D.; Abe-Hashimoto, J.; Su, M. J.; Felt, S.; Gibson, D. F. C.; Pillai, S. *J. Invest. Dermatol*. **1995**, *105*, 693.
44. Farach-Carson, M. C.; Abe, J.; Nishii, Y.; Khoury, R.; Wright, C.; Norman, A. W. *Am. J. Physiol*. **1993**, *265*, F705.
45. Takeyama, K.; Masuhiro, Y.; Fuse, H.; Endoh, H.; Murayama, A.; Kitanaka, S.; Suzawa, M.; Yanagisawa, J.; Kato, S. *Mol. Cell. Biol*. **1999**, *19*, 1049.
46. Geller, D. S.; Farhi, A.; Pinkerton, N.; Fradley, M.; Moritz, M.; Spitzer, A.; Meinke, G.; Tsai, F. T.; Sigler, P. B.; Lifton, R. P. *Science* **2000**, *289*, 119.
47. Peleg, S.; Sastry, M.; Collins, E. D.; Bishop, J. E.; Norman, A. W. *J. Biol. Chem*. **1995**, *270*, 10551.
48. van den Bemd, G. J. C. M.; Pols, H. A. P.; Birkenhager, J. C.; van Leeuwen, J. P. T. M. *Proc. Natl. Acad. Sci. U.S.A*. **1996**, *93*, 10685.
49. Konno, K.; Maki, S.; Fujishima, T.; Liu, Z.; Miura, D.; Chokki, M.; Takayama, H. *Bioorg. Med. Chem. Lett*. **1998**, *8*, 151.
50. Umesono, K.; Murakami, K. K.; Thompson, C. C.; Evans, R. M. *Cell* **1991**, *65*, 1255.